Available online at www.sciencedirect.com
SCIENCE DIRECT
Journal of Power Sources 151 (2005) 79–84
JOURNAL OF POWER SOURCES
www.elsevier.com/locate/jpowsour

Short communication

Carbon supports for methanol oxidation catalyst

P.V. Samant [a], C.M. Rangel [b,*], M.H. Romero [b], J.B. Fernandes [c], J.L. Figueiredo [a]

[a] *Laboratório de Catálise e Materiais, Departamento de Engenharia Química, Faculdade de Engenharia da Universidade de Porto, Rua Dr Roberto Frias, 4200-465 Porto, Portugal*
[b] *Electroquímica de Materiais, UEQM, Departamento de Materiais e Tecnologias de Produção, INETI, Paço do Lumiar, 1649-038 Lisboa, Portugal*
[c] *Department of Chemistry, Goa University, Taleigao, Plateau, Goa 403206, India*

Accepted 28 February 2005
Available online 24 May 2005

Abstract

Highly mesoporous carbon was synthesized employing conventional sol–gel technique using resorcinol and formaldehyde. The porous carbon electrodes were characterized by X-ray powder diffraction, N_2 adsorption isotherm, atomic absorption spectroscopy (AAS). Platinum was anchored on support by the incipient wetness method and reduced to its metallic form using sodium formate as a reducing agent. The electrocatalysis for methanol oxidation on carbon supported Pt in acid and alkaline solutions were investigated. It was found that the activity of Pt for methanol oxidation was higher in alkaline than in acid medium. High mesopore surface area of carbon can significantly increase the metal dispersion and affect particle size, which favoured the progress of the electrochemical processes occurring during methanol oxidation.

Keywords: Mesoporous carbon; Electrocatalysts; Methanol oxidation; Direct methanol fuel cells

1. Introduction

In spite of the intense research efforts in the last decade, the lack of efficient and inexpensive electrocatalysts remains one of the challenges to the implementation of low temperature fuel cells [1,2].

Methanol oxidation at platinum based electrodes have been extensively studied in a fuel cells context and is still a subject of interest [3–8], with the applicability of platinum based electrodes restricted due to the accumulation of surface poisoning intermediates, such as CO, leading to loss of activity with time [9].

Poisoning phenomenon can be avoided by alloying platinum with oxophilic metals, such as Ru, Sn, etc. in bimetallic systems [10,11]. Ternary and quaternary Pt-Ru based catalysts are also used: PtRuOs, PtRuW, PtRuMo, PtRuSnW or PtRuOsIr, etc. [12–16]. V, Ni, Fe, Co and Cr oxides have been also investigated for their suitability for methanol oxidation [17–20], as they are less expensive and also possess active sites for the formation of oxy-species. Ni, NiO, nickel-modified manganese oxide or Pt–Ni have been employed [10,19,20]. In recent years, perovskite oxides have been studied as potential materials because they offer surface basicity character, which affect the oxidative dehydrogenation steps in methanol oxidation, and are stable particularly in alkaline medium [21].

A different approach, such as the one used in this work, investigates alternative materials to say Vulcan XC 72, quite often used in fuel cells, as a catalyst support.

Recently, platinum nanoparticles on carbon nanotubes have been investigated as supports for cathode catalyst in direct methanol fuel cells (DMFC) [22]. Zeolites are also found to be efficient bringing about efficient diffusion of the reactants and or the products from its surface during the reaction [23,24]. Nanoporous TiO_2 has also found to be an effective support for the oxidation of methanol [25].

Supports have been found to possess strong influence on the particle size and the dispersion of the metal. The present investigation aims at preparing a highly mesoporous carbon.

* Corresponding author. Tel.: +351 21 0924657; fax: +351 21 7166568.
E-mail address: carmen.rangel@ineti.pt (C.M. Rangel).

0378-7753/$ – see front matter © 2005 Elsevier B.V. All rights reserved.
doi:10.1016/j.jpowsour.2005.02.083

Presence of surface groups on these materials along with their pore size can be exploited in the area of electrocatalysis of DMFC.

2. Experimental

2.1. Preparation and characterisation of the carbon support

High-density carbon xerogel were synthesized by condensation of the 1,3-dihydroxybenzoic acid and formaldehyde in a molar ratio of 2:1 using aqueous solution of sodium carbonate under sub-critical temperature conditions. The gel was cured at 27, 50 and 90 °C, for 1 day at each temperature. The water from the gel was removed by using different low volatile organic solvents, such as acetone and cyclohexane. The carbonisation of the gel was carried out in nitrogen atmosphere at 800 °C. The sodium present was removed by soxhlet extraction in 2 M HCl. The carbon obtained is hereafter referred to as CX.

The porous structures of the carbon xerogel were measured by N_2 adsorption desorption isotherm using 100CX Omnisorb coultometer. The *t*-method was applied for evaluation of the mesopore surface area S_{meso}, the micropore volume V_{micro}, while S_{micro} and L (average micropore width) were calculated using Dubinin equations. X-ray powder diffraction of the samples were done using Cu Kα radiation of wavelength $\lambda = 1.54065$ for 2θ values between 20° and 90°.

EDAX was used to assess, qualitatively and in a first instance, the amount of Pt in the samples. The percentage of the metal content of the platinum on the carbon was quantitatively determined using Atomic Absorption Spectrometer model number GBC 906A using arc acetylene flame.

The total amount of the oxygen-containing surface groups present on CX was determined by temperature programmed desorption (TPD-MS), described in detail in reference [26], as well as TGA and elemental analysis.

2.2. Catalyst and catalyst layer preparation

Anchoring of platinum, 10 wt% Pt on CX, was prepared by the incipient wetness method. The reduction of the incorporated platinum catalyst was carried out by slow addition of 0.1 M sodium formate at 60 °C. The catalyst was washed with hot water and dried. The catalyst is hereafter referred to as 10PtCX.

For the catalyst layer preparation, a paste was made using 5% Nafion solutions and isopropyl alcohol, mixed under ultrasonic bath for 15 min. The obtained thick ink was evenly spread over toray carbon paper and dried in an oven at 110 °C for 1 h. The geometric surface area of the electrodes was 1–1.2 cm^2, having 10 mg of catalyst containing 1 mg of metal. Results were compared with catalyst layers with the same amount of catalyst using Vulcan XC-72R carbon from Electrochem. Inc., referred to as 10PtC.

A polycrystalline Pt rod with an area of 0.196 cm^2 was also used in order to locate more clearly the potential domain for the oxidation of methanol. Characterisation of the electrode was done by assessing the electrochemical active area of the electrode using cyclic voltammetry.

2.3. Electrochemical characterisation

Cyclic voltammograms (CV) of the catalyst layers were recorded in sulphuric acid solution using an EG&G PAR Potentiostat/Galvanostat model 273 A. Before the experiment, the potential was repeatedly scanned in the same range at the scan rate of 75 mV s^{-1} till a reproducible voltammogram was obtained. Finally, the CV's were produced at the scan rate of 5 mV s^{-1}. Solutions were de-aerated with nitrogen. The reference electrode used was saturated calomel electrode (SCE) and a flag of platinum foil served as counter electrode. The catalytic activity was measured by potentiodynamic polarisation curves with sweep rate of 10 mV s^{-1} in 0.5 M CH_3OH and either 0.5 M H_2SO_4 or 0.5 M KOH at 298 K, respectively. The potential is referred to as that of normal hydrogen electrode (NHE).

3. Results and discussion

3.1. Textural characterisation

The nitrogen adsorption isotherm on to 10PtCX and CX, shown in Fig. 1, is a typical curve representative of type IV according to the BDDT classification. The steep rise in the adsorption of N_2 at $P/P_0 \leq 0.5$ indicated the presence of mesopores in carbon. The mesopore surface area was found to decrease upon the introduction of metal Pt on the support CX, which indicates impregnation or anchoring of metal particles inside mesopores of the carbon. This behaviour is also accompanied by decrease in BET surface area as well as a decrease in micropore volume, see Table 1. A BET area of

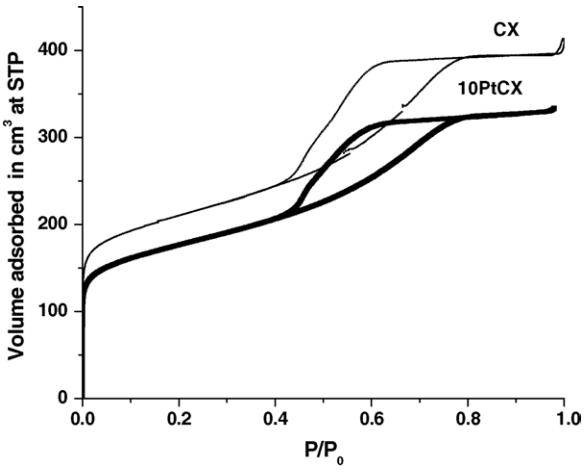

Fig. 1. Nitrogen adsorption isotherm for 10PtCX and CX at 77 K.

Table 1
Textural properties of 10PtCX and CX by nitrogen adsorption isotherm and temperature programmed desorption studies (TPD)

Sample	BET ($m^2\,g^{-1}$)	S_{meso} ($m^2\,g^{-1}$)	V_{micro} ($cm^3\,g^{-1}$)	L (nm)	CO_2 ($\mu mol\,g^{-1}$) (TPD)	CO ($\mu mol\,g^{-1}$) (TPD)
CX	724	524	0.11	0.70	216	709
10PtCX	630	396	0.095	1.24	–	–

Table 2
Comparison between % of metal by AAS and EDX, and particle size by XRD and electrochemical method of 10PtCX and 10PtC samples

Catalyst	Nominal wt% Pt	AAS (wt%)	EDAX[d] (wt%)	[a]XRD D(1 1 1) (nm)	[b]XRD D(2 2 0) (nm)	[c]D (nm)	a_{fcc} (Å)
10PtCX	10	7.9	8.5	1.91	2.80	1.15	3.9
10PtC	10	–	8.0	–	–	1.99	–

[a] Average particle size calculated from XRD at (1 1 1) reflection.
[b] Average particle size calculated from XRD at (2 2 0) reflection.
[c] Particle size from electrochemical measurement between 0 and 0.3 V vs. NHE a_{fcc}-lattice parameter.
[d] Qualitative.

$724\,m^2\,g^{-1}$ for the synthesized carbon contrast with an area for Vulcan XC-72R of $\sim 250\,m^2\,g^{-1}$.

Further, the metal composition was measured using AAS and EDAX. Results are within the nominal weight percent of platinum on the carbon as reported in Table 2. Particle size is reported to be ~2 nm. X-ray diffraction patterns of the catalysts 10PtCX and CX were obtained and shown Fig. 2. 10PtCX exhibited the characteristics peaks for the planes (1 1 1), (2 0 0), (2 2 0) and (3 1 1) at 2θ values of 39.770, 46.111, 67.621 and 81.401, respectively. These are associated to the diffraction peaks of the FCC structure typical of platinum (JCPDs, card 4-802). The average particle size was determined using peak $2\theta = 39.77$ and 67.621, corresponding to (1 1 1) (for comparing it with electrochemical measurements) and (2 2 0) reflection of FCC structure (the range where the diffraction spectrum of the carbon support only contributes in terms of linear background), by employing the Scherrer equation,

$$D = \frac{k\lambda}{\beta \cos\theta} \quad (1)$$

where λ is 1.54056 Å and β = FWHM (width of diffraction peak at half maxima in radians of 2θ) [27], value is reported in Table 2.

The lattice parameter, a_{fcc}, was evaluated from the angular position of the (1 1 1) peak maxima, according to

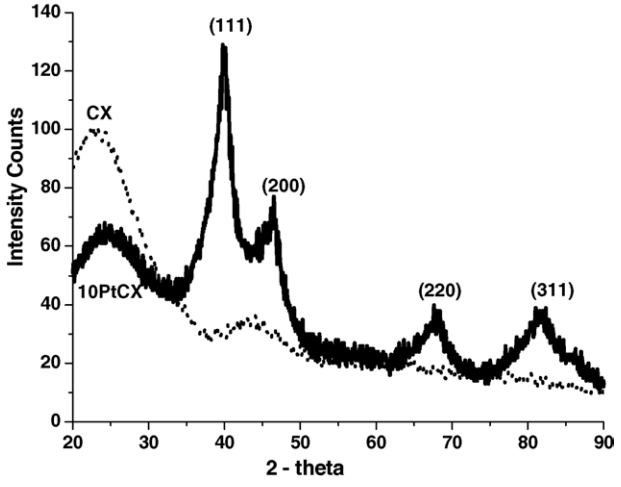

Fig. 2. XRD patterns for supported catalyst 10PtCX and high surface area carbon CX.

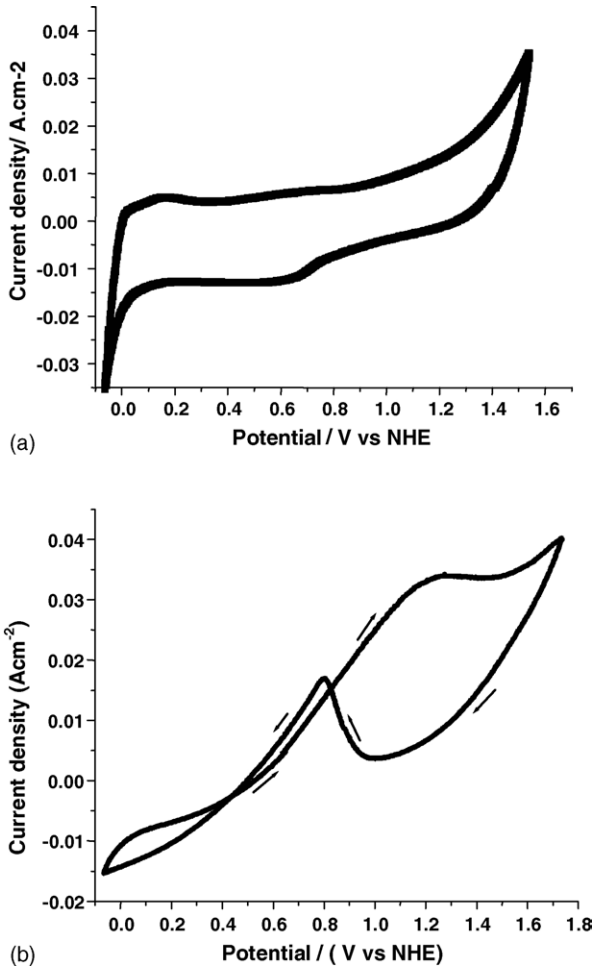

Fig. 3. Voltammograms for the electrode 10PtCX in (a) 0.5 M H_2SO_4; (b) 0.5 M H_2SO_4 + 0.5 M CH_3OH, scan rate of 5 mV s^{-1}.

Eq. (2),

$$a_{\mathrm{fcc}} = \frac{\lambda(h^2 + k^2 + l^2)^{1/2}}{2\sin\theta_{hkl}} \quad (2)$$

The metal surface area S_{Pt} was also obtained form the XRD mean particle size using the equation,

$$S_{\mathrm{Pt}} = \frac{6000}{\rho_{\mathrm{Pt}} \times D} \quad (3)$$

where $\rho_{\mathrm{Pt}} = 21.4\ \mathrm{g\,cm^{-3}}$. The mean particle size (D) was determined by comparing XRD, and from electrochemically active surface area, assuming that $1\ \mathrm{cm^2}$ of smooth platinum requires $210\ \mu\mathrm{C}$ of charge in the hydrogen adsorption/desorption region. This was done for both synthesised carbon and Vulcan XC-72R, see Table 2.

3.2. Electrochemical characterisation

In Fig. 3a, it is shown the cyclic voltammogram for 10PtCX in 0.5 M H_2SO_4 solution, registered at a scan rate of $5\ \mathrm{mV\,s^{-1}}$ at 298 K. The voltammogram is typical of high surface area carbon supported electrodes [5]. Note the poor definition of the peaks in the hydrogen adsorption/desorption region. There is indication of oxygen reduction suggesting that the solution is only partially de-aerated. The kinetics of the h.e.r (using a logarithmic scale for the current) shows good linearity and Tafel values in agreement with the literature.

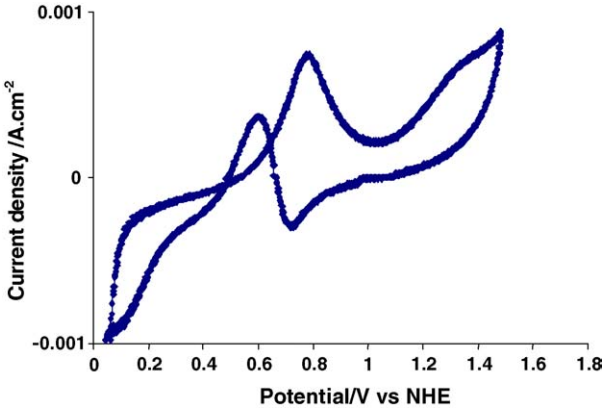

Fig. 4. Voltammogram for bulk polycrystalline platinum in $H_2SO_4 + CH_3OH$, showing well resolved peaks peak in the anodic branch and a clear reduction peak before methanol re-oxidation in the reverse scan.

With methanol addition to the acid solution in a concentration of 0.5 M, the following features were observed, Fig. 3b:

- a marked increase in the anodic current due to the dehydrogenation of methanol followed by oxidation of adsorbed intermediaries, possible reactions are:

$$CH_3OH + Pt_{(s)} \rightarrow Pt\text{–}CH_2OH_{ads} + H^+ + e^- \quad (4)$$

$$Pt\text{–}CH_2OH_{ads} + Pt_{(s)} \rightarrow Pt_2\text{–}CHOH_{ads} + H^+ + e^- \quad (5)$$

$$Pt_2\text{–}CHOH_{ads} + Pt_{(s)} \rightarrow Pt_3\text{–}COH_{ads} + H^+ + e^- \quad (6)$$

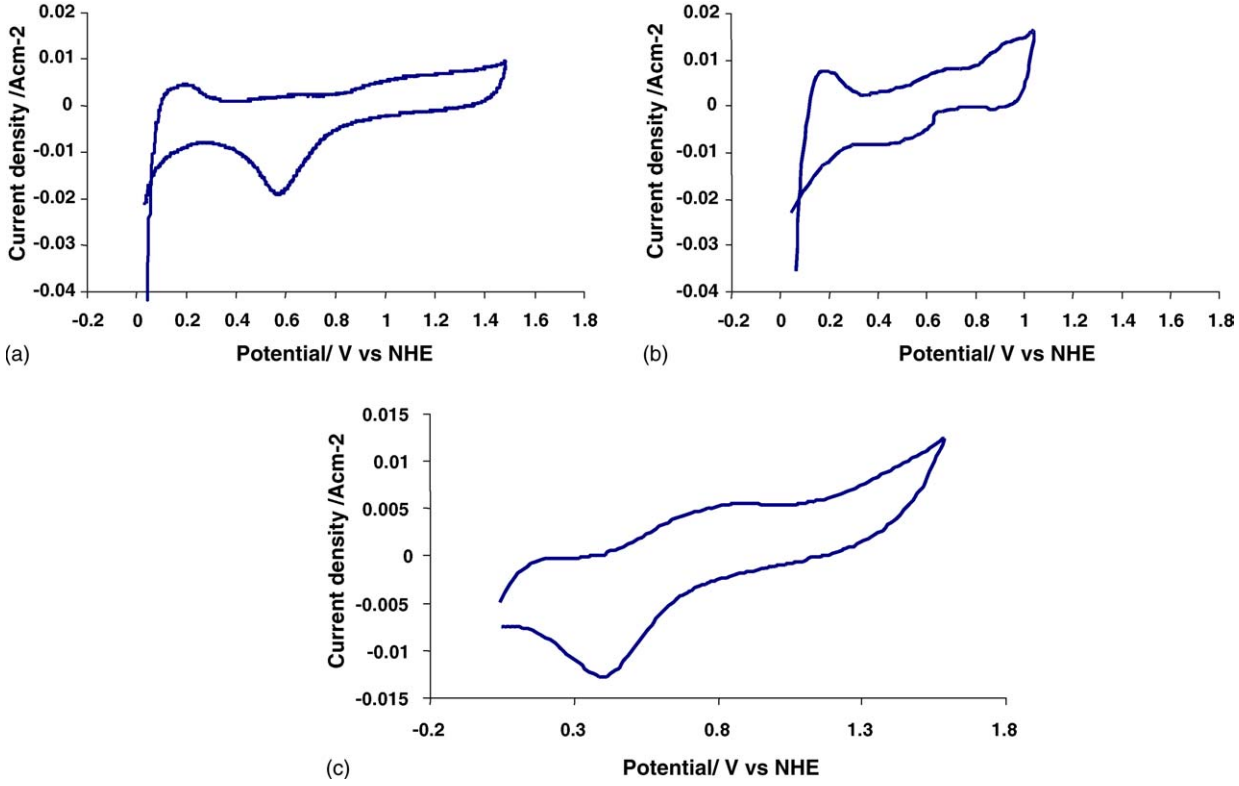

Fig. 5. Voltammogramss for electrodes 10PtC in (a) 0.5 M H_2SO_4; (b) 0.5 M H_2SO_4 + 0.5 M CH_3OH; (c) 0.5 M H_2SO_4 + 0.5 M CH_3OH after cycling.

$$Pt_3\text{–}COH_{ads} \rightarrow Pt\text{–}CO_{ads} + 2Pt_{(s)} + H^+ + e^- \quad (7)$$

The extension of the potential may include the formation of Pt oxides/hydroxides and oxidation of CO to CO_2, possible reactions are,

$$Pt_{(s)} + H_2O \rightarrow Pt\text{–}OH_{ads} + H^+ + e^- \quad (8)$$

$$Pt\text{–}CO + H_2O \rightarrow Pt\text{–}COOH_{ads} + H^+ + e \quad (9)$$

or

$$Pt\text{–}OH_{ads} + CO_{ads} \rightarrow Pt\text{–}COOH_{ads} \quad (10)$$

$$Pt\text{–}COOH_{ads} \rightarrow Pt_{(s)} + CO_2 + H^+ + e^- \quad (11)$$

- in the reverse scan a well defined peak is observed associated to methanol re-oxidation, which seem to be activated after the Pt oxides have been reduced, this is not evident at the shown scan rate;
- inhibition of the hydrogen adsorption/desorption region.

All of these features are more clearly distinguishable in the curves obtained with polycrystalline Pt, see Fig. 4.

Results were compared with those obtained using Pt electrodes supported on carbon Vulcan XC-72R, see Fig. 5, where the voltamograms exhibited lower current densities and a larger charge associated to the potential region attributed to the formation/reduction of Pt oxides/hydroxides at the used scan rates. Deactivation of the electrode for hydrogen absorption/desorption is evident after cycling, see Fig. 5b and c.

In alkaline solution (see Fig. 6), the oxidation of methanol follows desorption of H under potential deposition (UPD) and coincides with the potential for OH_{ads} (resulting from OH^- discharge in alkaline solution). However, for potentials higher than ($E > 1.1$ V), the platinum surface is highly covered by oxygenated species.

The pronounced current plateau (between 0.5 and 1.0 V) corresponds to a surface reaction in both acid and alkaline solution,

$$CO_{ads} + OH_{ads} \rightarrow CO_2 + H^+ + e^- \quad (12)$$

It appears that OH ions may act as a catalyst species. Platinum showed higher activity in alkaline medium as compared to acid which is in agreement with Tripkovic et al. [5]. One interesting feature noticed in alkaline medium is the effect of successive numbers of cycles. Voltammetric current corresponding to oxide formation gradually decreases with increasing cycle number and reaches a final state shown in Fig. 6b. This indicates that platinum surface slowly develops more favourable sites during cycling, similar phenomenon is observed in case of platinum deposited electrodes [28]. Fig. 6c shows stable voltammogram for the synthesized carbon CX in the absence of catalyst (five cycles).

During the oxidation of methanol in the absence of OH_{ads} species, products of the dehydrogenation of methanol can act as poison to deactivate the catalyst and inhibit the methanol reaction. Thus, oxidation of water and the ratio OH/H_2O regarding adsorption bond strengths, the activation energy for OH_{ads} formation, the ability to adsorb anions are factors affecting methanol oxidation [29,30]. Mechanism on dispersed porous carbon may be complex as reaction order changes with methanol concentration. Gojkavic and Vidakovic [31] reported that reaction (9) and (10) can occur simultaneously in parallel pathways.

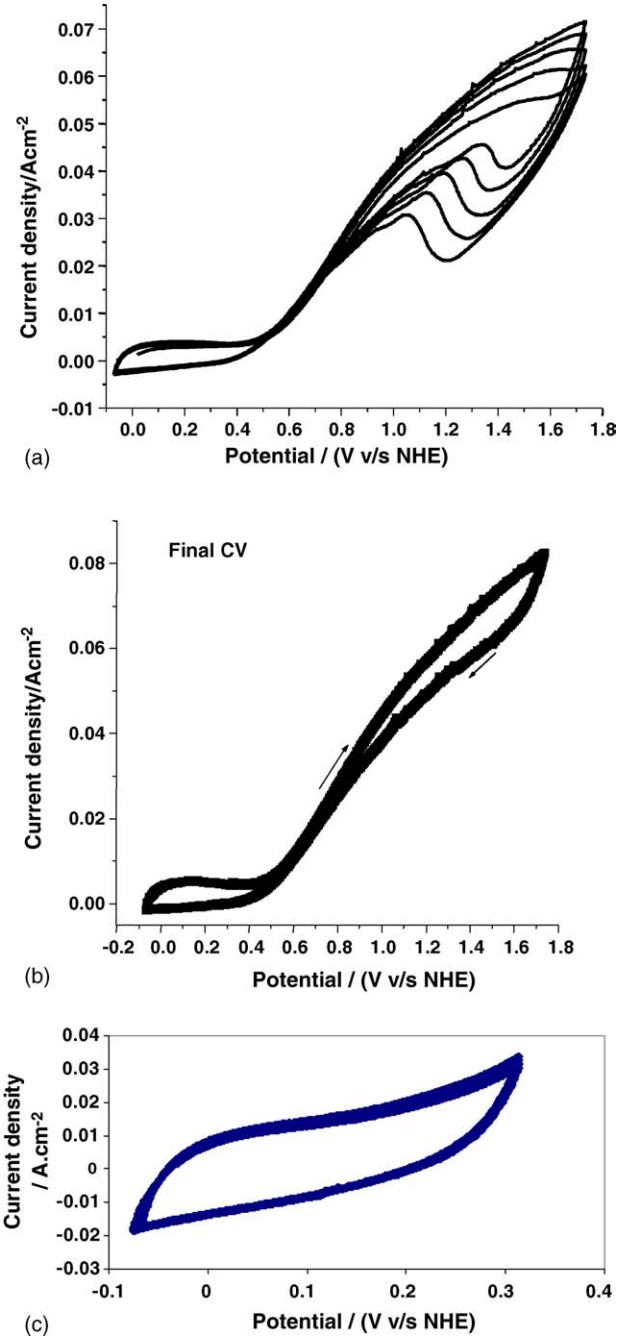

Fig. 6. Cyclic voltammogram in 0.5M CH_3OH and 0.5 M KOH solution at the scan rate of 5 mV s^{-1} (a) 10PtCX, 5 cycles at 27 °C; (b) 10PtCX after 10 cycles; (c) CX, 5 cycles.

Increase in the degree of dispersion may vary the number of different facets of platinum available for the electrocatalytic reaction. Methanol oxidation is highly favoured at low index platinum single-crystal faces such as Pt (1 1 1), due to facile oxidation CO to CO_2 [32,33]. For particle size larger than about 4 nm, plane (1 0 0) is favoured [31].

Also, the electronic interaction between carbon support through its large number of oxygenated surface groups (see also reference [26]), may be responsible for the attributed higher activity for methanol. The combination small particle crystallite with the carbon substrate tends to encourage the formation of OH_{ads} species necessary for promotion of the oxidation of the inhibiting intermediates during reactions in acid as well as in alkaline medium.

Further studies are necessary to elucidate the mechanism of methanol oxidation on supported catalyst.

4. Conclusions

- The carbon prepared through synthetic route presented large surface area, high mesoporosity and the presence of oxygenated surface groups required for methanol oxidation.
- Supported platinum showed higher electrocatalytic activity for methanol oxidation in alkaline medium than in acid solutions.
- Supported platinum PtCX shows better performance in the electro-oxidation of methanol than PtC for the same amount of catalyst.

Acknowledgements

This work was supported by Fundação para a Ciência e a Tecnologia (FCT/Portugal) under Programme POCTI/FEDER (POCTI/1181) and by the Indo-Portuguese Research Cooperation in Science and Technology.

References

[1] S. Wasumus, A. Kuver, J. Electroanal. Chem. 461 (1999) 14–31.
[2] G.J.K. Acres, J.C. Frost, G.A. Hards, R.J. Potter, T.R. Ralph, D. Thompsett, G.T. Burstein, G.J. Hutchings, Catal. Today 38 (1997) 393–400.
[3] A. Kucernak, J. Jiang, Chem. Eng. J. 93 (2003) 81–90.
[4] M. Umeda, M. Kokubo, M. Mohamedi, I. Uchida, Electrochim. Acta 48 (2003) 1367–1374.
[5] A.V. Tripkovic, K.D. Popovic, B.N. Grgur, B. Blinzanac, P.N. Ross, N.M. Markovic, Electrochim. Acta 47 (2002) 3707–3714.
[6] J.B. Goodenough, A. Hamnett, B.J. Kennedy, R. Manoharan, S.A. Weeks, Electrochim. Acta 35 (1990) 199–207.
[7] A. Maruyama, I. Abe, Electrochim. Acta 48 (2003) 1443–1449.
[8] M.S. Loffler, B. Groβ, H. Natter, R. Hempelmann, Th. Krajewski, J. Divisek, Phys. Chem. Chem. Phys. 3 (2001) 333–336.
[9] T. Iwasita, Electrochim. Acta 47 (2002) 3663–3674.
[10] U.A. Paulus, A. Wokaun, G.G. Scherer, T.J. Schmidt, V. Stamenkovic, N.M. Markovic, P.N. Ross, Electrochim. Acta 47 (2002) 3787–3798.
[11] A.S. Arico, H. Kim, A.K. Shukla, M.K. Ravikumar, V. Antonucci, N. Giordano, Electrochim. Acta 39 (1994) 691–700.
[12] K.L. Ley, R. Liu, C. Pu, Q. Fan, N. Leyarovska, C. Segre, E.S. Smotkin, J. Electrochem. Soc. 144 (1997) 1543–1548.
[13] C. He, H.R. Kunz, J.M. Fenton, J. Electrochem. Soc. 144 (1997) 970–979.
[14] Z. Jusys, T.J. Schmidt, L. Lasch, L. Jorissen, J. Garche, R.J. Behm, J. Power Sources 105 (2002) 297–304.
[15] E. Reddington, A. Sapienza, B. Gurau, R. Viswanathan, S. Sarangapani, E.S. Smotkin, T.E. Mallouk, Science 280 (1998) 1735–1737.
[16] B. Gurau, R. Vishwanathan, R. Liu, T.J. Lafrenz, K.L. Ley, E.S. Smotkin, J. Phys. Chem. B 102 (1998) 9997–10003.
[17] T. Ohmorie, K. Nodasaka, M. Enyo, J. Electroanal. Chem. 281 (1990) 331–337.
[18] A.K. Shukla, M. Neergat, P. Bera, V. Jayaram, M.S. Hegde, J. Electroanal. Chem. 504 (2001) 111–119.
[19] P.V. Samant, J.B. Fernandes, J. Power Sources 79 (1999) 114–118.
[20] J.F. Drillet, A. Ee, J. Friedemann, R. Kotz, B. Schnyder, V.M. Schmidt, Electrochim. Acta 47 (1988) 1983.
[21] V. Raghuveer, K.R. Thampi, N. Xanthopoulos, H.J. Mathieu, B. Viswanathan, Solid State Ionics 140 (2001) 263–274.
[22] W. Li, C. Liang, J. Qiu, W. Zhou, H. Han, Z. Wei, G. Sun, Q. Xin, Carbon 40 (2002) 787–803.
[23] P.V. Samant, J.B. Fernandes, J. Power Sources 125 (2004) 172–177.
[24] M. Shelef, U.S. Patent No. 6,117,581, September 12, 2000.
[25] B. Hayden, D.V. Malevich, D. Pletcher, Electrochem. Commun. 3 (2001) 395–399.
[26] P.V. Samant, F. Gonçalves, M.M.A. Freitas, M.F.R. Pereira, J.L. Figueiredo, Carbon 42 (2004) 1321–1325.
[27] V. Radmilpvic, H.A. Gasteiger, P.N. Ross Jr., J. Catal. 154 (1995) 98–106.
[28] C. Hu, K. Liu, Electrochim. Acta 44 (1999) 2727–2738.
[29] A.B. Anderson, Electrochim. Acta 47 (2003) 3759–3763.
[30] B.E. Conway, B.V. Tilak, Electrochim. Acta 47 (2002) 3571–3594.
[31] S.Lj. Gojkovic, T.R. Vidakovic, Electrochim. Acta 47 (2001) 633–642.
[32] N.M. Markovic, T.J. Schmidt, B.N. Grgur, H.A. Gasteiger, R.J. Behm, P.N. Ross, J. Phys. Chem. B 103 (1999) 8567–8577.
[33] N.M. Markovic, B.N. Grgur, C.A. Lucas, P.N. Ross, J. Phys Chem. B 103 (1999) 487–495.